

DOI: 10.1002/anie.200503797

**Finite-Size, Fully Addressable DNA Tile Lattices Formed by Hierarchical Assembly Procedures\*\****Sung Ha Park, Constantin Pistol, Sang Jung Ahn, John H. Reif, Alvin R. Lebeck, Chris Dwyer,\* and Thomas H. LaBean\**

The development of a versatile and readily programmable assembly system for the controlled placement of matter at the molecular scale remains a major goal for nanoscience, nanotechnology, and supramolecular chemistry. Herein, we present a significant step toward this goal by using self-assembling DNA nanostructures to construct fully addressable, finite-sized arrays displaying a variety of programmed patterns. We have assembled DNA tile arrays decorated with proteins in the shape of the letters “D”, “N”, and “A” that are less than 80 nm on a side. We demonstrate procedures that explore two extremes in hierarchical assembly strategies: 1) minimization of the number of unique molecular address labels (DNA sticky-end sequences) required for encoding tile associations, and 2) minimization of the depth (number of sequential steps) of the assembly process. Higher production yields of defect-free assemblies were achieved by procedures that minimize assembly depth (and maximize diversity of address labels). Some observations on scaling of these strategies to larger arrays are also presented.

[\*] Dr. C. Dwyer

Department of Electrical and Computer Engineering  
Duke University, Durham, NC 27708 (USA)  
Fax: (+1) 919-660-1605  
E-mail: [dwyer@ece.duke.edu](mailto:dwyer@ece.duke.edu)

Dr. T. H. LaBean

Departments of Computer Science and Chemistry  
Duke University, Durham, NC 27708 (USA)  
Fax: (+1) 919-660-1605  
E-mail: [thomas.labean@duke.edu](mailto:thomas.labean@duke.edu)

Dr. S. H. Park

Physics Department  
Duke University, Durham, NC 27708 (USA)C. Pistol, Dr. J. H. Reif, Dr. A. R. Lebeck  
Department of Computer Science  
Duke University, Durham, NC 27708 (USA)

Dr. S. J. Ahn

Length Laboratory  
Korea Research Institute of Standards and Science  
Daejeon, 305-340 (Korea)

[\*\*] We thank H. Yan and P. Yin for helpful discussions and J. Liu for the use of the DI Nanoscope IIIa AFM. This work was supported by grants from the National Science Foundation to T.H.L. (EIA-02-18376), J.H.R. (CCF-04-32038), and A.L. (CCR-03-26157). We are also grateful for support from the Duke University Provost Common Fund and Duke University Graduate School, and for equipment donations from IBM and Intel.

Supporting information for this article is available on the WWW under <http://www.angewandte.org> or from the author.

Fifteen years ago, Eigler and Schweizer made a significant advance in nanoscale construction when they used a scanning tunneling microscope (STM) to position 35 xenon atoms at precise sites on a nickel surface.<sup>[1]</sup> They wrote “IBM” in letters a mere 5 nm on an edge, thus presaging a variety of research applications such as quantum corrals and single-molecule chemistry. However, nanofabrication by STM requires expensive instruments under low-temperature, ultra-high-vacuum conditions and produces only one or a small number of copies of a desired structure. This last limitation restricts the applicability and scalability of STM and other top-down assembly methods such as e-beam lithography. Bottom-up self-assembly, on the other hand, can be used to fabricate huge numbers of objects simultaneously, but previous demonstrations of molecular-scale self-assembly lacked sufficient programming complexity to form objects as sophisticated as letters. Herein, we report massively parallel fabrication (on the order of  $10^{13}$  copies) of letters less than 80-nm square by DNA-based self-assembly.

Self-assembled nanostructures with DNA as building blocks were proposed by Seeman in 1982<sup>[2]</sup> and recently have been experimentally demonstrated in a wide variety of forms.<sup>[3]</sup> DNA nanostructures have been assembled by using carefully designed linear oligonucleotides with complementary base-pairing segments that form branch-junction motifs. These assemblies were produced with various geometrical structures and functionalities: one- and two-dimensional periodically patterned structures,<sup>[4–12]</sup> three-dimensional polyhedra,<sup>[13–15]</sup> nanomechanical devices,<sup>[16–21]</sup> molecular computers,<sup>[22–26]</sup> and organizations of other functionalized molecules.<sup>[27–29]</sup> DNA's excellent intrinsic characteristics, which include molecular recognition, programmability, self-organization, and molecular-scale structuring properties, make it an interesting nanoscale building material, although up to now its usefulness in nanotechnology applications has been limited by a lack of finite-size control and unique addressability in the assembled objects. Finite-sized assemblies have been prototyped with cleverly designed RNA puzzle pieces, and have been shown to form objects with the potential for symmetric addressability,<sup>[30]</sup> although their use for the display of any arbitrary 2D pattern has not yet been demonstrated.

Herein, we report the prototype fabrication of size-controllable, fully addressable, and precisely programmable DNA-based nanoarrays (NAs) consisting of cross-shaped tiles by using a novel stepwise hierarchical assembly technique. We implemented the construction of fully addressable, finite-size “ $N$  (row)  $\times$   $M$  (column)” NAs from DNA tiles with four arms, each of which contains a Holliday junction-like crossover;<sup>[7,8]</sup> these DNA tiles are referred to here as “cross tiles”. DNA nanostructures were visualized by atomic force microscopy (AFM) under buffer solution, and their dimensions were shown to be in excellent agreement with the designs. The fixed-size DNA nanostructures described may find future use as templates for organizing heteromaterials for developing nanotechnologies, especially in nanoelectronics including, but not limited to, fabrication of functionalized nanowires,<sup>[31]</sup> nanocircuits,<sup>[32]</sup> quantum cellular automata,<sup>[33]</sup> and spintronic devices.<sup>[34]</sup>

Perhaps the simplest strategy for the construction of finite-sized nanostructures with maximal control over the placement of components would be to use unique DNA sequences everywhere throughout the structure. Such a design would necessarily restrict the maximum allowable size of the structure because of limitations on the size of the set of unique DNA sequences available. Herein, we made use of stepwise assembly strategies that involve the sequential buildup of hierarchical superstructures, such that the formation of stable substructures allows the reuse of DNA base sequences that are complemented and sequestered within double-helical domains. We investigated a “minimal sequence set” (MSS) assembly strategy, which makes maximal reuse of sticky-end sequences and requires a four-step procedure for assembly of a 16-tile,  $4 \times 4$  lattice (Figure 1 B). We compared this procedure with a “minimal depth” (MD) assembly strategy, which reduces the number of assembly steps by reusing base sequences only at the tile cores and by using unique sequences for all sticky ends encoding tile-to-tile associations. The MD strategy required the redesign of each of the five-base-pair sticky ends (two per arm) to satisfy the constraint that each tile should match perfectly at only one position in the 16-tile lattice.<sup>[35]</sup> This second strategy allows the construction of a  $4 \times 4$  NA in a two-step process (Figure 1 C).

Schematic diagrams of the self-assembling cross tiles are shown in Figure 1 A. The drawings show simplified strands as colored lines that represent different DNA strands, with arrowheads marking the 3' ends. Each tile consists of three kinds of strands: a central loop strand, four shell strands, and four arm strands. The arm strands carry five-base sticky ends at both the 5' and 3' ends. Both construction strategies make use of two different core sequences (A and B tile types, see red/blue diagrams in Figure 1 B and C), which are defined by the loop and shell strands. Detailed core nucleotide sequences and sets of complementary sticky ends for tile associations are given in the Supporting Information.

Schematics of the strategies and AFM imaging results of the MSS and MD assembly procedures for 16-tile  $4 \times 4$  NAs are given in Figure 1 B and C, respectively. The MSS strategy begins with eight test tubes containing two tiles each (Figure 1 B, i), then it proceeds to four tubes of four tiles (Figure 1 B, ii), two tubes of eight tiles (Figure 1 B, iii), and finally one tube containing all 16 tiles (Figure 1 B, iv). The MD strategy requires one step of 16 tubes with one tile each (Figure 1 C, i), followed immediately by a second step with one tube containing all 16 tiles (Figure 1 C, ii).

Our stepwise assembly technique is a general method for the construction of any finite-size  $N \times M$  NA. For example,  $2 \times 2$  NAs (Figure 1 B, ii) were fabricated in two steps: in the first annealing step, equimolar mixtures of the strands for tiles 1 and 2 were placed in one tube and strands for tiles 3 and 4 were mixed in a separate tube. These were then cooled slowly from 95 to 20 °C, and then in the second step (low-temperature anneal) equal volumes of the two  $1 \times 2$  NAs were mixed and cooled slowly from 42 to 20 °C by floating the microtube in 1 L of water at 42 °C, which was then cooled to room temperature on the bench over  $\approx 4$  h. Low-temperature annealing prevents the assembled supertiles and lattices from

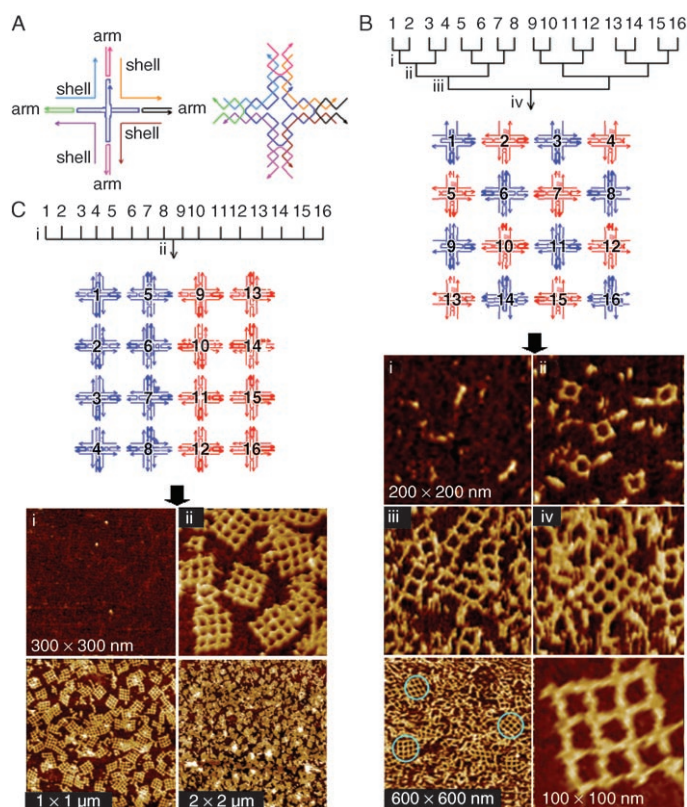


**Figure 1.** DNA tile and NA structures and assembly schemes. A) Schematic drawings of the strand trace in cross tiles with strand names marked (arm, shell, and loop). B) MSS strategy and constructs. A converging-stream diagram of the four-step assembly process starting with eight tubes of two tiles each (i) and concluding with one tube containing all 16 tiles (iv). The blue and red diagram shows the placement of tiles (1 through 16) in the NA and the identity of loop strands (A-loops are blue and B-loops are red). The bottom six panels are AFM height images with dimensions as labeled and height scale from 0 to 3 nm. Panels i)–iv) correspond to the same labels as in the annealing scheme above; thus, i)  $1 \times 2$  NA, ii)  $2 \times 2$  NA, iii)  $2 \times 4$  NA, and iv)  $4 \times 4$  NA. The two bottom AFM images are zoom-out and zoom-in pictures of (iv), with error-free NAs in the zoom-out image circled in turquoise. C) MD strategy and constructs. A converging-stream diagram of the two-step assembly starts with 16 tubes with one tile each (i) and goes directly to one tube of 16 tiles (ii). The blue and red diagram shows the placement of A-loop and B-loop tiles in the final NA. The bottom four panels are AFM height images with i) showing single tiles and ii) showing complete  $4 \times 4$  NAs. The two bottom panels are zoom-out images to show the increased production yield of defect-free assemblies from the two-step method.

dissociating into their component tiles or strands. In this case, the melting temperature for the component cross tiles is  $\approx 60^\circ\text{C}$ .<sup>[7]</sup> As the five-base sticky ends average 50% CG content, their melting temperatures are expected to be  $\approx 30^\circ\text{C}$ , so reheating them to  $42^\circ\text{C}$  provided sufficient structural motion to facilitate further hybridization to the desired lattice structures. Subsequent assembly steps involved reheating to a moderate temperature (below the expected melting point of any desired substructure), followed by slow cooling back to room temperature. This is the process used in the sequential steps outlined in Figure 1B. Similarly, the MD assembly (Figure 1C) also required reheating of the 16-tile mixture to  $23^\circ\text{C}$  and then slow cooling to room temperature

over the course of 4 h. Incubation of annealed samples at  $4^\circ\text{C}$  overnight prior to examination by AFM improved the quality of the imaging data.

Comparison of the AFM scans in Figure 1B and C reveals that the two-step process produces higher yields of properly assembled target structures and fewer partially assembled “waste” products. We define the production yield of defect-free assemblies as the proportion of the total mass of material observed that is found in well-formed target structures. We analyzed the AFM images and counted single tiles,  $1 \times 2$ ,  $2 \times 2$ , and all other NAs and lattice fragments. We estimated production yields by tallying the total numbers of target structures and fragments, multiplying each tally by the object size in units of whole tiles (as whole tiles are the smallest observable substructure), and dividing the number of cross tiles found in the target structures by the total number of cross tiles observed in the AFM images. By analyzing several scans of wide areas from several different annealing reactions we can estimate the production yield for each assembly strategy. The first step of the MSS assembly procedure results in a  $1 \times 2$  NA with average yields of approximately  $0.80 \pm 0.04$ . We estimate a production yield of about  $0.11 \pm 0.03$  for the final  $4 \times 4$  NA in the MSS assembly. On the other hand, the two-step MD assembly strategy results in production yields of approximately  $0.34 \pm 0.06$  for the  $4 \times 4$  NA structure. To effectively utilize stepwise strategies with multiple assembly steps in the future, and to increase the yield of final products, it is desirable to maximize the yield and purity of the target structure at each step. This may require the adoption of purification steps to remove unassociated and/or misassembled strands that could interfere downstream.

We tested our ability to properly address the NAs by including loop strands modified with biotin at desired points in the assembly process. Binding of individual streptavidin (SA) molecules at biotin sites generates bumps (height  $\approx 5$  nm) at the center of the cross tiles. The lattices can be thought of as pixel arrays, and in these experiments the binding of SA protein at a given grid point corresponds to the pixel being turned on, whereas the absence of SA represents a pixel in the off state. Figure 2A shows high-resolution AFM images of a variety of programmed patterns on  $2 \times 2$  NAs, which demonstrate the full addressability of the constructs. The images show symmetrically and asymmetrically patterned SA and clearly demonstrate the successful assembly of  $2 \times 2$  NAs with the MSS system.

The programming of  $4 \times 4$  NAs was demonstrated by using both MSS and MD assembly schemes. Figure 2B shows diagrams and high-resolution AFM images of three different  $4 \times 4$  NAs with programmed deletions produced by the MSS strategy. These partial arrays demonstrate not only the addressability and programmability of the  $4 \times 4$  NAs, but also the rigidity and robustness of the structure. Another example of MSS-programmed fabrication shown in Figure 2C is of NAs with biotin–SA conjugates on all eight of its B tiles (the 100-nm scan shows the detail and the 800-nm scan gives an idea of the construction yield). Figure 2D and E show

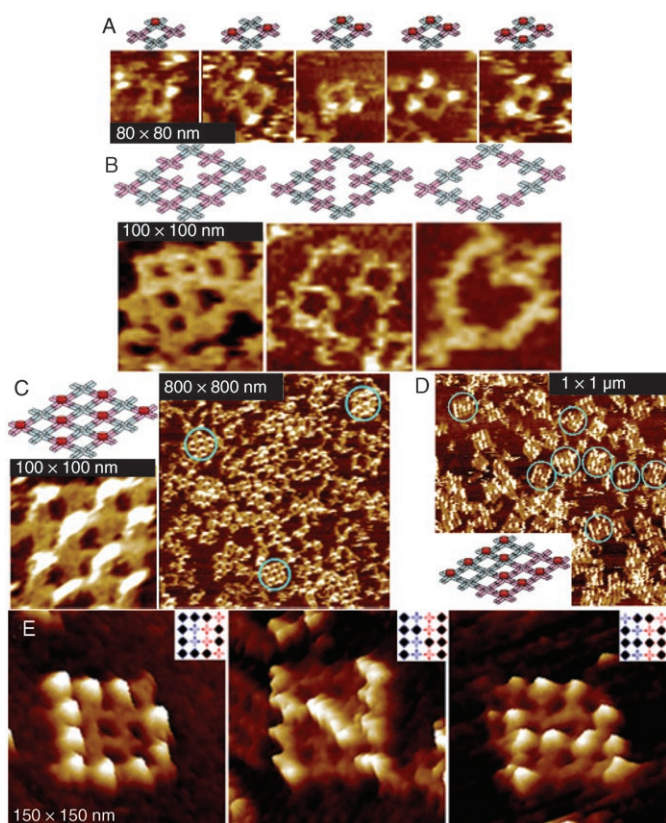


**Figure 2.** Demonstration of precise programming by self-assembly. A) Diagrams and AFM height images of  $2 \times 2$  NAs with programmed SA protein attachment. B) Diagrams and AFM images of  $4 \times 4$  NAs assembled by the MSS strategy and displaying programmed holes. Left: without tile 6; middle: without tiles 6 and 11; and right: without tiles 6, 7, 10, and 11 (see also Supporting Information). C) Diagram and AFM images of a minimal-sequence  $4 \times 4$  NA programmed with a specific SA protein pattern. The zoom-out scan shows a mixture of final products with error-free arrays circled in turquoise. D) Diagram and AFM image of a  $4 \times 4$  NA assembled by the MD process and displaying a specific pattern with defect-free arrays circled in turquoise. E) The letters “D”, “N”, and “A” displayed on self-assembled  $4 \times 4$  arrays by the two-step MD strategy.

schematics and AFM images of assemblies produced with the MD system and programmed to display specific patterns that resemble the letters D, N, and A. Based on the observed production yields of the letter “D” and the sample volume and concentration, we estimate that the procedure generated on the order of  $10^{13}$  copies of the target nanostructure. The success of these self-assembly procedures lends credence to a wide range of proposed molecular self-assembly fabrication schemes. By balancing the reuse of DNA sequences (MSS strategy) with the number of assembly steps (MD strategy) to achieve an acceptable production yield, we can begin to place bounds on the size of the 2D DNA tile lattices that we can reasonably hope to construct. We also examined the scaling of the required number of sticky-end sequences and the depth (number of sequential steps) of the assembly process with increasing NA dimensions (see the Supporting Information).

In summary, we have designed and assembled size-controlled and fully addressable DNA-based nanoarrays in

a hierarchical stepwise manner. The reliability of stepwise assembly and the molecular-level control demonstrated by our system represents a major step toward developing DNA-based nanotechnologies for myriad future applications. Potential uses include fixed-size algorithmic assemblies for DNA computing and complex patterning of nanomaterials for the fabrication of artificial bionanomachines, devices, and sensors. By prototyping the two extremes of assembly strategy—minimal sequence set and minimal process depth—we have begun to experimentally investigate the ranges of production yield and the limits on object size that we can hope to achieve by self-assembly using DNA tile nanofabrication.

### Experimental Section

The design of cross-tile types A and B was based on the structure of immobile four-arm branched junctions. The subsequence used for all bulged loops was T4. Sequences were designed with the program SEQUIN<sup>[36]</sup> to minimize the chance of undesired complementary association and sequence symmetry. Synthetic oligonucleotides were purchased from Integrated DNA Technologies (Coralville, IA) and purified by polyacrylamide gel electrophoresis. Complexes were formed by mixing a stoichiometric quantity of each strand in physiological buffer,  $1 \times \text{TAE/Mg}^{2+}$  (Tris acetate (40 mM, pH 8.0), EDTA (2 mM), and magnesium acetate (12.5 mM)). The final concentration of DNA was between 0.0625 and 1.0  $\mu\text{M}$ . In the first annealing step, equimolar mixtures of strands were heated to 95°C, cooled slowly to 20°C by placing the Eppendorf tubes in 2 L of boiled water in a styrofoam box for at least 40 h to facilitate hybridization, and then incubated overnight at 4°C for structure stabilization. In subsequent steps, moderate-temperature annealing was performed by cooling the DNA tile mixtures slowly from 42°C (40°C for the third step and 38°C for the fourth step) to 20°C by placing the Eppendorf tubes in 1 L of water on the bench for  $\approx 4$  h. The samples were incubated overnight at 4°C after each annealing step. Biotinylated loop strands and SA interaction were used to demonstrate full addressability. SA was added to the aqueous solution of the assembled NAs for 1 h at room temperature. The final concentration of SA was between 0.0625 and 1.0  $\mu\text{M}$ , and matched the concentration of biotinylated loop strands. The samples were incubated overnight at 4°C before AFM imaging.

AFM was performed in the tapping mode under  $1 \times \text{TAE/Mg}^{2+}$  buffer. An annealed sample (5  $\mu\text{L}$ ) was dropped onto freshly cleaved mica and left for 5 min. A portion of  $1 \times \text{TAE/Mg}^{2+}$  buffer (30  $\mu\text{L}$ ) was then placed on the mica and another portion (30  $\mu\text{L}$ ) was placed on the AFM tip. AFM images were obtained on a Digital Instruments Nanoscope IIIa instrument with a multimode fluid-cell head by using NP-S oxide-sharpened silicon nitride tips (Veeco).

Received: October 27, 2005

Published online: December 22, 2005

**Keywords:** DNA structures · nanostructures · nanotechnology · self-assembly · supramolecular chemistry

[1] D. M. Eigler, E. K. Schweizer, *Nature* **1990**, *344*, 524.

[2] N. C. Seeman, *J. Theor. Biol.* **1982**, *99*, 237.

[3] N. C. Seeman, *Nature* **2003**, *421*, 427.

[4] E. Winfree, F. Liu, L. A. Wenzler, N. C. Seeman, *Nature* **1998**, *394*, 539.

[5] C. Mao, W. Sun, N. C. Seeman, *J. Am. Chem. Soc.* **1999**, *121*, 5437.

- [6] T. H. LaBean, H. Yan, J. Kopatsch, F. Liu, E. Winfree, J. H. Reif, N. C. Seeman, *J. Am. Chem. Soc.* **2000**, *122*, 1848.
- [7] H. Yan, S. H. Park, G. Finkelstein, J. H. Reif, T. H. LaBean, *Science* **2003**, *301*, 1882.
- [8] S. H. Park, P. Yin, Y. Liu, J. H. Reif, T. H. LaBean, H. Yan, *Nano Lett.* **2005**, *5*, 729.
- [9] D. Liu, S. H. Park, J. H. Reif, T. H. LaBean, *Proc. Natl. Acad. Sci. USA* **2004**, *101*, 717.
- [10] D. Liu, M. Wang, Z. Deng, R. Walulu, C. Mao, *J. Am. Chem. Soc.* **2004**, *126*, 2324.
- [11] B. Ding, R. Sha, N. C. Seeman, *J. Am. Chem. Soc.* **2004**, *126*, 10230.
- [12] Y. Brun, M. Gopalkrishnan, D. Reishus, B. Shaw, N. Chelyapov, L. Adleman, *Proceedings of the 1st Conference on the Foundations of Nanoscience* **2004**, pp. 2–15.
- [13] J. Chen, N. C. Seeman, *Nature* **1991**, *350*, 631.
- [14] Y. Zhang, N. C. Seeman, *J. Am. Chem. Soc.* **1994**, *116*, 1661.
- [15] W. M. Shih, J. D. Quispe, F. Gerald, G. F. Joyce, *Nature* **2004**, *427*, 618.
- [16] C. Mao, W. Sun, Z. Shen, N. C. Seeman, *Nature* **1999**, *397*, 144.
- [17] B. Yurke, A. J. Turberfield, A. P. Mills, F. Simmel, J. L. Neumann, *Nature* **2000**, *406*, 605.
- [18] H. Yan, X. Zhang, Z. Shen, N. C. Seeman, *Nature* **2002**, *415*, 62.
- [19] L. Feng, S. H. Park, J. H. Reif, H. Yan, *Angew. Chem.* **2003**, *115*, 4478; *Angew. Chem. Int. Ed.* **2003**, *42*, 4342.
- [20] J. J. Li, W. Tan, *Nano Lett.* **2002**, *2*, 315.
- [21] W. U. Dittmer, A. Reuter, F. C. Simmel, *Angew. Chem.* **2004**, *116*, 3634; *Angew. Chem. Int. Ed.* **2004**, *43*, 3550.
- [22] L. Adleman, *Science* **1994**, *266*, 1021.
- [23] E. Winfree, *J. Biomol. Struct. Dyn.* **2000**, *18*, 263.
- [24] C. Mao, T. H. LaBean, J. H. Reif, N. C. Seeman, *Nature* **2000**, *407*, 493.
- [25] Y. Benenson, T. Paz-Elizur, R. Adar, E. Keinan, Z. Livneh, E. Shapiro, *Nature* **2001**, *414*, 430.
- [26] B. Ravinderjit, N. Chelyapov, C. Johnson, P. Rothmund, L. Adleman, *Science* **2002**, *296*, 499.
- [27] C. M. Niemeyer, W. Bürger, J. Peplies, *Angew. Chem.* **1998**, *110*, 2391; *Angew. Chem. Int. Ed.* **1998**, *37*, 2265.
- [28] J. J. Storhoff, C. A. Mirkin, *Chem. Rev.* **1999**, *99*, 1849.
- [29] S. E. Baker, W. Cai, T. L. Lasseter, K. P. Weidkamp, R. J. Hamers, *Nano Lett.* **2002**, *2*, 1413.
- [30] A. Chworos, I. Severcan, A. Koyfman, P. Weinkam, E. Oroudjev, H. Hansma, L. Jaeger, *Science* **2004**, *306*, 2068.
- [31] E. Braun, Y. Eichen, U. Sivan, G. Ben-Yoseph, *Nature* **1998**, *391*, 775.
- [32] C. Dwyer, L. Vicci, J. Poulton, D. Erie, R. Superfine, S. Washburn, R. Taylor, *IEEE Trans. on VLSI* **2004**, *12*, 1214.
- [33] M. Lieberman, S. Chellamma, B. Varughese, Y. Wang, C. Lent, G. Bernstein, G. Snider, F. Peiris, *Ann. N. Y. Acad. Sci.* **2002**, *960*, 225.
- [34] M. Zwolak, M. Di Ventra, *Appl. Phys. Lett.* **2002**, *81*, 925.
- [35] C. Dwyer, S. H. Park, T. H. LaBean, A. R. Lebeck, *Proceedings of the 2nd Conference on the Foundations of Nanoscience, Vol. 2*, **2005**, p. 187.
- [36] N. C. Seeman, *J. Biomol. Struct. Dyn.* **1990**, *8*, 573.